
<https://doi.org/10.15407/ujpe63.11.957>

A.V. TURCHIN

Institute of Physics, Nat. Acad. of Sci. of Ukraine
(46, Prosp. Nauky, Kyiv 03028, Ukraine; e-mail: turchin@iop.kiev.ua)

“IN-GAP” SPECTROSCOPY: REFLECTED-WAVE PHASE AND FILM CHARACTERIZATION

Optical methods that are used to characterize the state of a surface covered with films are based on the measurement of either the ratio between the complex reflection coefficients for mutually orthogonal light polarizations (ellipsometry) or the magnitudes of reflection coefficients themselves; afterward, the parameters of films such as their number, thicknesses, and transparencies can be determined by the fitting, while solving the corresponding inverse problem. In order to extend the set of quantities that can be measured experimentally, a method is proposed that allows the phase of the reflected light wave to be determined, by analyzing the spectral features for light reflected from a plane-parallel gap between the surface of analyzed specimen and upper window. In particular, the spectrum obtained, by using the “moving specimen” procedure, can be transformed into the spectral dependences of the magnitude and phase of the reflection coefficient. As a result, the inverse problem of finding the dielectric permittivity of a single-layer film is reduced to the solution of a linear matrix equation, which makes the proposed method more advantageous in comparison with the ellipsometric one, for which there is no direct relationships between the ellipsometric angles and the physical parameters of the film.

Keywords: interferometry, wave phase, surface characterization, inverse problem.

1. Introduction

A variety of single- and multilayer films that differ from one another by their chemical compositions and creation methods is typical of practically every modern technology. Those films include relatively simple anticorrosion or antireflection coatings, multilayer dielectric mirrors, and coatings with specific (and controlled) photosensitive, catalytic, photo-catalytic, magnetic, and other properties. These are also modern complex devices for the information storage and transmission, in which multilayer films with a complicated architecture of every layer are applied, as a rule [1].

Requirements to the quality and accuracy of the film fabrication become more and more severe and generate the challenge to develop new methods for characterizing the parameters and properties of the films at every stage of technological process, proceeding from the development and research of the films with new properties to the development of a film deposition technology and, finally, the monitoring of the fabrication process (preferably, *in-situ*). Among the methods of nondestructive film control (with a possibility to use *in-situ* diagnostics), optical methods of characterization became very important. As a rule, they are aimed at determining both the film thickness d_{film} and the spectral dependence of the complex refractive index $N(\nu) = n(\nu) + i\kappa(\nu)$, where

$n(\nu)$ and $\kappa(\nu)$ are the dependences of the refractive index and the absorption index, respectively, on the wave number ν . The results of such measurements allow the phase state of the film (amorphous or crystalline), the phase ratio (e.g., rutile/anatase in the case of titanium dioxide), the film surface roughness, the porosity (if a homogeneous film is grown with the help of a pore-forming material), the semiconductor band-gap width, and the type of optical transition in the semiconductor (direct or indirect) to be evaluated [2, 3].

The kit of applied optical methods became rather stable during a long period of their usage. The methods described below do not include refractometers of various types, because their automatization in order to measure spectral dependences is difficult.

- Sometimes, when the dielectric permittivity of a bulk substance (or a film with a known thickness) is determined, the absorption coefficient is calculated first from the spectral data obtained for the coefficients of light reflection and transmission. Afterward, the real part of the dielectric permittivity is found by using the Kramers–Krönig relations [4, 5]. A significant shortcoming of this method is a necessity for measuring the film absorption in the middle and far ultraviolet range.

- The spectra of the light energy reflection, $R(\nu)$, and transmission, $T(\nu)$, coefficients have an oscillatory character for films owing to the interference between the waves reflected from the both film sides. The extrema in the both dependences approximately correspond to the resonance and antiresonance of reflected waves. In order to specify the position of extrema, the transcendental equations, which involve the monotonic character of the dependences $n(\nu)$ and $\kappa(\nu)$, have to be solved in the general case. A film characterization procedure with the help of approximate relationships for the extrema was described in works [6–8]. Experiments of this type are attractive owing to their simplicity: it is enough to measure any of the dependences, $R(\nu)$ or $T(\nu)$. But they have at least two shortcomings. Firstly, in the case of thin films with the thickness $d < 0.5 \mu\text{m}$, the number of extrema is too small. Therefore, exact relationships have to be used when determining the spectral dependences. Moreover, the information about the $R(\nu)$ or $R(\nu)$ dependence in the intervals between the extrema is also desirable. Secondly, even in the case of a homogeneous single layer, the mea-

surement data obtained for only one quantity describing the transformation of light energy are not enough to determine two dependences, $n(\nu)$ and $\kappa(\nu)$. Therefore, there arises a necessity for measuring the spectral dependence of the amplitude reflection coefficient $r(\nu)$ ($R(\nu) = |r(\nu)|^2$), which describes both the magnitude and the phase of a reflected wave.

- The films of amorphous semiconductors are sometimes characterized by fitting experimental data obtained for $R(\nu)$ or $T(\nu)$ with the help of a model function for the dielectric permittivity of a semiconductor [9–11].

- Various kinds of ellipsometry (multiple-angle monochromatic ellipsometry, spectral ellipsometry, etc.) are considered to be the most reliable and exact methods [12–16]. Experimentally measured are the ellipsometric angles $\Psi(\nu)$ and $\Delta(\nu)$, which are related to the ratio of the complex amplitude reflection coefficients $r_p(\nu)$ and $r_s(\nu)$ for the p - and s -polarized waves, respectively, by the formula

$$\frac{r_p(\nu)}{r_s(\nu)} = \tan \Psi(\nu) \exp[i\Delta(\nu)].$$

A unique advantage of ellipsometry is its ability to provide information about the difference $\Delta(\nu)$ between the phases of the reflected waves with the p - and s -polarizations.

The available optical methods were developed rather long ago and can characterize films quite well. However, to our knowledge, none of them can be used to measure the phase of each of the amplitude coefficients separately. The development of a method for the measurement of the spectral dependences of those phases is the main purpose of this work. The knowledge of the phases makes it possible to completely restore the complex coefficients $r_p(\nu)$ and $r_s(\nu)$, thus supplying the maximally full information about the specular reflection from any surface. One should expect that the information completeness will be especially useful for reproducing the physical properties of films and clean surfaces (the solution of the inverse problem) in complicated cases, since the database for calculations will be significantly extended. These may be systems, in which reflection is modulated by external factors (e.g., an inverse layer near the semiconductor surface), or systems with a complicated (and unusual) spectral dependence of the reflected wave phase (e.g., surface plasmons). Finally, these may be systems, in which the boundary conditions

for light reflection are more complicated than those for an isotropic dielectric film considered in this work (e.g., anisotropic films, systems with excited excitons or any other additional waves, and so forth).

Another purpose of this work consists in studying whether the information completeness is also useful in the case of simple systems. Namely, whether experimental data concerning only the reflection spectrum are enough or not for a complete solution of the inverse problem in the case of a thin single-layer film.

The structure of the paper is as follows. In Section 2, an idea of the method for measuring the phase of the amplitude reflection coefficient is explained. In Subsection 3.1, the method is illustrated by a reflectance spectrum calculated in a typical case of the thin film of a model semiconductor. A numerical analysis of the spectrum is described in Subsection 3.2. A general idea of solution of the inverse problem is discussed in Subsection 3.3. Subsection 3.4 demonstrates how this solution can be implemented on the basis of only the reflection spectrum data. Calculation details are given in Appendix.

2. Idea of the Method

By definition, the phase of the amplitude reflection coefficient is the difference between the phases of the incident and reflected waves at the surface. In principle, in order to measure this difference, it is enough to make the both waves interfere. That will do for the direct phase measurements in the radio frequency range. In the optical spectral range, there arises a problem to relate the measured optical signal intensity with the phase difference of interfering waves.

When comparing various methods for the determination of the phase difference (the interference phases), it should be noted that a single measurement of the intensity is not enough to extract the phase difference, because the signal intensity also depends on the wave magnitudes. Therefore, there emerges the necessity for multiple measurements, for which the phase difference varies by at least 2π . Significant progress in the experiments of this type can be achieved provided that a coherent light source is used. For instance, in the case of digital holographic microscopy (DHM) [17–19], there arises a monochromatic two-dimensional pattern of interference between the examined optical front and a plane reference beam. An analysis of this picture following

a special algorithm [20] allows the distributions of both the front amplitude and phase to be extracted from the set of spatial measurements.

In the case of scanning near-field optical microscopy (SNOM), a monochromatic field that is formed by the diffraction at small structures is tested with the help of an optical fiber tip. The latter supplies light to one of the fiber interferometer arms [21]. In the heterodyne variant of this method [22], the frequency-shifted reference signal is supplied to the other arm, and the magnitude and phase of the optical field at a certain point in the space are determined by heterodyning the total signal, i.e. by analyzing how the set of interference measurements changes in time. The spatial field distribution is measured by scanning it with the help of the fiber tip, so that the resolution of the method exceeds the diffraction limit.

Numerous methods of phase shift interferometry [23–26] were developed to evaluate the shape and roughness of optical surfaces or to profile microelectronic objects. They are based on the set of monochromatic interference measurements that arises when the phase shift along the reference arm of an interferometer is controllably varied by displacing the mirror or the diffraction grating, rotating the glass etalon plate, changing the laser frequency, or rotating the polarization devices.

At the same time, the profiling interferometry techniques such as coherent scanning interferometry or optical coherent tomography [27–29] use low-coherent (“white light”) sources and the modulation of reference arm length. Actually, they measure the distance to certain surface fragments rather than the phase of the field, because the interference signal is observed, only if the optical path difference does not exceed the light coherence length.

Even this simplified review of interferometric phase measurement methods demonstrates that they are strongly different, and their application depends on the measurement purpose and conditions. At the same time, they do not provide the measurement of the interference phase in a more or less wide spectral interval. In this paper, we show that the stated goal can be achieved, by using only a set of spectral measurements. The main idea of the proposed method consists in creating the interference of the incident and reflected light beams with a constant optical path difference between them. In this case, the additional interference oscillations are imposed

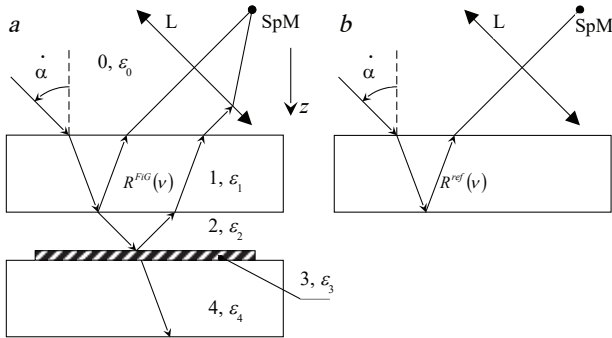


Fig. 1. The “Film-in-Gap” structure: schematic diagrams of the reflection spectrum (a) and reference spectrum (b) measurements: (0) external environment (air, $\varepsilon_0 = 1$); (1) transparent window with the dielectric permittivity ε_1 ; (2) plane-parallel air gap with the thickness d_2 and the dielectric permittivity $\varepsilon_2 = \varepsilon_0 = 1$; (3) film with the thickness d_3 and the dielectric permittivity ε_3 ; (4) substrate with the dielectric permittivity ε_4

on the oscillations in the surface reflection spectrum (e.g., these are oscillations of the film reflection coefficient $R(\nu)$ associated with the film thickness and described in Introduction). The period of new oscillations is determined by the optical path difference and can be made arbitrarily short to trace the features in the $R(\nu)$ spectrum. The exact value of their phase is unambiguously related to the phase of the amplitude reflection coefficient for the film-covered surface, $r_{\text{film}}(\nu)$.

The structure proposed for the implementation of this idea is depicted in Fig. 1, a. It can be called the “Film-in-Gap” (FiG) structure. The plane-parallel air gap 2 of the thickness $d_{\text{gap}} = d_2$ is formed from one of its sides by film 3 characterized by the thickness $d_{\text{film}} = d_3 \ll d_2$ and the dielectric permittivity $\varepsilon_{\text{film}}(\nu) = \varepsilon_3(\nu)$. The film is deposited onto transparent substrate 4. From the other side, the gap is confined by transparent window 1. The light beam falls on the structure at the angle α . The reflected light is focused by lens L at the light guide inlet and is directed to spectrometer SpM. Below, for simplicity, we assume that

- the dielectric permittivity of air $\varepsilon_0 = 1$;
- the window and the substrate are made of the same transparent isotropic material, so that $\varepsilon_4(\nu) = \varepsilon_1(\nu)$ and $\text{Im} \varepsilon_1 = 0$;
- the film is optically isotropic and, in a certain spectral interval, absorbing, i.e. $\text{Im} \varepsilon_3 \geq 0$;
- the incident wave is *s*-polarized.

From the experimental viewpoint, this optical scheme has a number of advantages. In the case of light reflection at a substantial angle with respect to the normal and provided that the substrate and the window are sufficiently thick, there appears a possibility to separate the beam that is coherently reflected by three closely located interfaces (window-gap, gap-film, and film-substrate) from other two beams that are reflected by external sides of the structure and carry no significant information (Fig. 1, a). The spectral dependence of the separated beam intensity will be denoted by $R^{\text{FiG}}(\nu)$. In addition, the reflection spectrum can be conveniently and accurately normalized on the basis of the “moving specimen” principle. For this purpose, it is enough to remove the substrate together with the film and measure the reference reflection spectrum $R^{\text{ref}}(\nu)$ (Fig. 1, b) without changing the lens and fiber optic guide positions.

The main advantage of this scheme consists in that the phase of the wave reflected from the structure manifests itself in the experimental reflection spectrum $R^{\text{FiG}}(\nu)$ as short-period oscillations, which are convenient for the numerical analysis. Note also that the gap sides form an asymmetric Fabry–Perot interferometer, and the lower side of the window plays the role of a beam mixer. The light reflected from the latter is a superposition of the incident beam and the beam reflected by the film, with the superposition coefficients depending only on the refractive index of the window material and the gap thickness.

The exact solution of the problem of *s*-polarized light transmission through an arbitrary layered structure is presented in a compact form in Appendix. Using expressions (D5) and (D6) for the reference reflection amplitude $y_{\text{win}}^{\text{ref}}(z_2, \nu)$ and the reflection amplitude $y_{\text{win}}^{\text{FiG}}(z_2, \nu)$ for the FiG structure, respectively, we obtain the following relation between the normalized reflection spectrum of the structure, $\rho(\nu)$, and the reflection amplitude $r_{\text{film}}(\nu)$ from an arbitrary film (in the general case, from an arbitrary surface):

$$\rho(\nu) = \frac{R^{\text{FiG}}(\nu)}{R^{\text{ref}}(\nu)} = \frac{\left| y_{\text{win}}^{\text{FiG}}(z_2, \nu) \right|^2}{\left| y_{\text{win}}^{\text{ref}}(z_2, \nu) \right|^2} = \frac{1 + r_{12}^{-2} |r_{\text{film}}(\nu)|^2 + 2r_{12}^{-1} |r_{\text{film}}(\nu)| \cos \beta(\nu)}{1 + r_{12}^2 |r_{\text{film}}(\nu)|^2 + 2r_{12} |r_{\text{film}}(\nu)| \cos \beta(\nu)}. \quad (1)$$

The spectral dependence of the reflection amplitude from the window-gap interface, $r_{12}(\nu)$, is considered

to be a known function. The phase of short-period spectral oscillations

$$\beta(\nu) = \arg(r_{\text{film}}(\nu)) + 4\pi\nu d_2 \sqrt{\varepsilon_0} \cos \alpha \quad (2)$$

differs from the phase of the coefficient of reflection from the film $\varphi(\nu) = \arg(r_{\text{film}}(\nu))$ only by a term that linearly depends on the wave number ν . This circumstance makes it possible, by processing the experimental reflection spectrum, to find not only the magnitude $m(\nu) = |r_{\text{film}}(\nu)|$, but also the phase $\varphi(\nu)$ of the complex amplitude reflection coefficient of the film, $r_{\text{film}}(\nu) = m(\nu) \exp[i\varphi(\nu)]$, and thus to completely restore this parameter.

Hence, spectrum (1) contains as much information as possible about the specular light reflection at the angle α from a film on a substrate. As far as we know, this is currently the only experimental method with the described capabilities. This fact distinguishes it from other experimental methods, in which only a piece of the required information can be extracted. It is evident that the additional experimental possibilities make it possible to pose new problems and propose new solutions for old ones. In so doing, the specific methods and procedures of data processing can vary depending on the research purpose, the quality of experimental data, and so on. For instance, in the next section, a new approach to the "eternal" inverse problem of finding the dielectric permittivity of a thin single-layer semiconductor film is proposed.

3. Numerical Calculations for a Single-Layer Film

The calculations, which results are presented below, were carried out not only to illustrate the proposed method, but also to demonstrate the procedure of solution of the inverse problem: how the amplitude reflection coefficient of the film $r_{\text{film}}(\nu)$ and, afterward, the film thickness d and dielectric permittivity $\varepsilon_{\text{film}}(\nu)$ can be calculated, by using only the normalized reflection spectrum of the FiG structure $\rho(\nu)$. The solution accuracy provided by numerical procedures is an important factor. Therefore, in Subsection 3.1, the reflection spectrum is calculated in the typical case of a thin single-layer amorphous semiconductor film. The spectrum imitates data that can be measured experimentally and serves as a basis for the further solution of the inverse problem. The analysis of this spectrum is described in Subsection 3.2. It

allows the film reflection magnitude $|r_{\text{film}}(\nu)|$ and the phase of short-period oscillations $\beta(\nu)$ to be extracted. The procedure of calculation of the film thickness, as well as the spectral dependences $r_{\text{film}}(\nu)$ and $\varepsilon_{\text{film}}(\nu)$ for the known gap thickness, is described in Subsection 3.3. Finally, the procedure of refinement of the gap thickness is described in Subsection 3.4.

3.1. "Film-in-Gap" reflection spectrum

Two requirements were stipulated for model calculations, which results are summarized below. First, these results should correspond as much as possible to a possible experimental data in the optical spectral interval corresponding to wave numbers $\nu = 1 \div 3 \mu\text{m}^{-1}$, which draws enhanced attention. Second, it would be desirable to demonstrate the asymptotic behavior of the spectrum at low frequencies, $\nu \rightarrow 0$, focusing special attention on the phases of the short-period spectrum and the amplitude reflection coefficient of the film. Unfortunately, this requirement takes us beyond the validity scope of expressions that approximate the refractive index of optical materials. However, in the case of demonstration calculations, such an extrapolation seems to be acceptable.

Fused quartz is a typical material for the fabrication of the window and the substrate. Its transparency interval extends from the near IR to the middle UV range [5]. In this interval, its dielectric permittivity is described by the Sellmeier formula, which coefficients were published in work [30]. When calculating the model spectrum of the quartz refractive index $n_{fs}(\nu)$, only two terms in the formula were used. The third term describing the absorption in the middle IR range was omitted. It is important that the omitted term has little effect on the results obtained for the spectral interval that attracts experimental interest.

In calculations, we assumed that a semiconductor film of amorphous TiO_2 with the thickness $d_{\text{film}} = d_3 = 0.15 \mu\text{m}$ was deposited on the substrate. When calculating the absorption spectrum, the dielectric properties of the film, according to the Forouhi-Bloomer approximation [9, 10], were approximated by the following expression:

$$\kappa_{\text{film}}(\nu) = \begin{cases} 0, & \nu < \nu_g, \\ \frac{A(\nu - \nu_g)^2}{\nu^2 - B\nu + C}, & \nu \geq \nu_g, \end{cases} \quad (3)$$

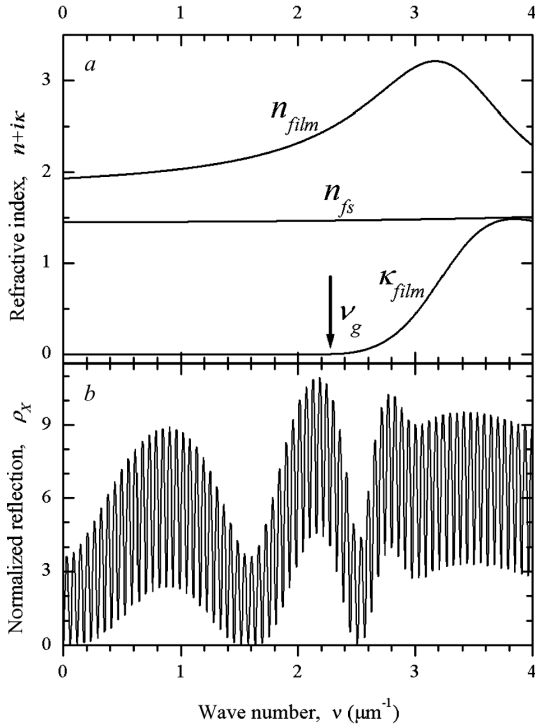


Fig. 2. Spectra of the model refractive and adsorption indices for the substrate, $n_{fs}(\nu)$, and the film, $n_{film}(\nu)$ and $\kappa_{film}(\nu)$ (a). Normalized reflection spectrum of the “Film-in-Gap” structure $\rho_X(\nu)$ (b)

where ν_g is the wave number corresponding to the semiconductor bandgap width. The values of the parameters A , B , and C depend on the position, width, and strength of the electron transition. In order to satisfy the Kramers–Krönig relations, the spectrum of the refractive index has to be expressed by the following formula:

$$n_{film}(\nu) = n_\infty + \frac{B_0\nu + C_0}{\nu^2 - B\nu + C}, \quad (4)$$

where the coefficients B_0 and C_0 are algebraic functions of the parameters in expression (3). Numerical values of all required parameters were calculated from experimental data in work [9]. In calculations, the model dielectric permittivity of the semiconductor film was approximated by the following expression:

$$\varepsilon_3(\nu) = \varepsilon_{film}(\nu) = N_{film}^2(\nu) = (n_{film}(\nu) + i\kappa_{film}(\nu))^2. \quad (5)$$

The spectral dependences $\kappa_{film}(\nu)$ and $n_{film}(\nu)$ together with the model spectrum for the refractive in-

dex of fused quartz $n_1(\nu) = n_4(\nu) = n_{fs}(\nu)$ are shown in Fig. 2, a. The exact calculation procedure for the FiG reflectance spectrum is described in Appendix [see expressions (D7) and (D8)], and the results of calculation of the normalized spectrum $\rho_X(\nu)$ are exhibited in Fig. 2, b. The subscript X emphasizes that this spectrum simulates experimental data for the procedures described below.

The whole reflection spectrum contains approximately three oscillations owing to the small film thickness. This fact emphasizes once more that it is difficult to make substantiated conclusions about the properties of thin films solely on the basis of their reflection spectra. However, owing to the created FiG structure, there arose short-period oscillations, which period is exclusively governed by the gap thickness $d_{gap} = d_2 = 10 \mu\text{m}$. The rate of phase growth $d\beta/d\nu$ along the spectral interval varies by a few percent. Therefore, the oscillation period remains almost constant and practically independent of the dielectric permittivity and thickness of the film.

In the calculated spectrum, the amplitude of short-period oscillations remains large in the high-frequency interval as well. This is not so for the experimental spectrum. Due to the ordinary experimental factors (the spectrometer line width, appreciable angular spectrum of the probe light, small deviations of the gap sides from the planeness and parallelism), the amplitude of those oscillations decreases, as the frequency grows. Therefore, when processing the spectrum, it is reasonable to use only the phase of short-period oscillations and the averaged reflection parameter. This method of processing of the spectrum is considered in the next section.

3.2. Reflection magnitude and short-period oscillation phase

The processing of the “experimental” spectrum $\rho_X(\nu)$ is aimed at separating its rapidly oscillating component from a slowly varying background. This procedure is incorrect in the general case. However, a rather good approximation can be obtained, if the gap thickness strongly exceeds the film thickness. It is also worth noting that the presence of oscillating terms in the numerator and denominator of expression (1) makes the numerical processing more difficult. It is more convenient to introduce a new spectral variable $w_X(\nu)$, which is a homographic function

of the spectrum $\rho_X(\nu)$:

$$w_X(\nu) = \frac{1 + r_{12}^2 \rho_X}{1 - r_{12}^2 \rho_X} \frac{1 - r_{12}^2}{1 + r_{12}^2}. \quad (6)$$

According to formula (1), its dependence on the film reflection magnitude $m(\nu)$ and the short-period oscillation phase $\beta(\nu)$ has the simplest form

$$\begin{aligned} w_X(\nu) &= \frac{1 + m^2}{1 - m^2} + \frac{4r_{12}m}{(1 - m^2)(1 + r_{12}^2)} \cos \beta(\nu) = \\ &= w_m(\nu) + w_a(\nu) \cos \beta(\nu). \end{aligned} \quad (7)$$

Expression (7) also contains the slowly varying spectral functions $w_m(\nu)$ and $w_a(\nu)$. Their obvious meaning is the average values of the function $w_X(\nu)$ and the amplitude of its oscillation, respectively.

The spectral dependence $w_X(\nu)$ calculated by formula (6) is shown in Fig. 3, *a*. The dependence $w_m(\nu)$ was extracted, by numerically processing the spectrum $w_X(\nu)$ with the help of the local regression method followed by the low-frequency Fourier filtering. Then the quantity $(w_X(\nu) - w_m(\nu))^2$ was constructed, and its processing with the use of the same regression-filtration method made it possible to extract the dependence $w_a(\nu)$. The result of filtration is depicted in Fig. 3, *a* in the form of combinations $w_m(\nu) + w_a(\nu)$ and $w_m(\nu) - w_a(\nu)$. The both curves approximate the local extrema of the dependence $w_X(\nu)$ very well, which testifies to a good extraction accuracy of the oscillating spectral component.

Finally, the processing of the "experimental" spectrum $\rho_X(\nu)$ terminates after the extraction of two dependences: the film reflection magnitude

$$m_X(\nu) = \sqrt{\frac{w_m(\nu) - 1}{w_m(\nu) + 1}} \quad (8)$$

and the phase of short-period oscillations $\beta_X(\nu)$, which satisfies the formula

$$\cos \beta_X(\nu) = \frac{w_X(\nu) - w_m(\nu)}{w_a(\nu)}. \quad (9)$$

Attention should be paid to the low-frequency asymptotic behavior of the spectra, $\rho_X(\nu \rightarrow 0) \rightarrow 0$ and $w_X(\nu \rightarrow 0) \rightarrow w_m(\nu) - w_a(\nu)$, and the phase, $\beta_X(\nu \rightarrow 0) \rightarrow \pi$. This is an expected result, if the wavelength significantly exceeds the gap and film thicknesses, and the film does not absorb, $\kappa_{\text{film}}(\nu \rightarrow 0) = 0$.

3.3. Calculation of the dielectric permittivity of a single-layer film

Suppose that we know the gap thickness d_{gap} . In this case, the solution of the inverse problem can be constructed in the following way. First, using formula (2), we find the phase $\varphi_X(\nu)$ of the film reflection coefficient,

$$\varphi_X(\nu) = \beta_X(\nu) - 4\pi\nu d_{\text{gap}} \sqrt{\varepsilon_0} \cos \alpha. \quad (10)$$

The plots of the dependences $m_X(\nu)$ and $\varphi_X(\nu)$ are depicted in Fig. 3, *b*. Now, the spectral dependence

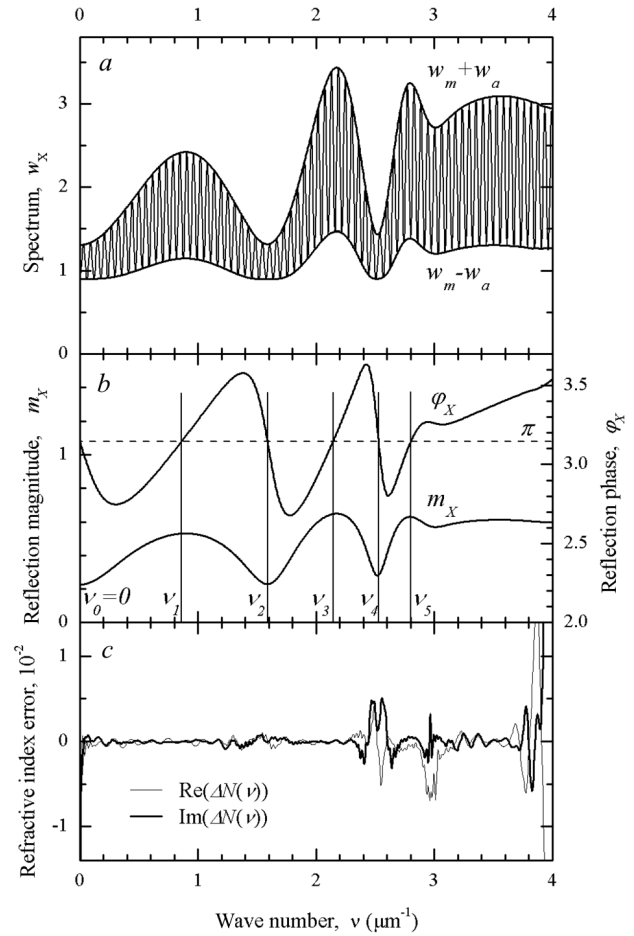


Fig. 3. Inverse problem solution. Oscillating spectral dependence $w_X\nu$ calculated by formula (6) (*a*). Slowly varying spectral functions $w_m(\nu) + w_a(\nu)$ and $w_m(\nu) - w_a(\nu)$ approximate the local extrema of the dependence $w_X(\nu)$ calculated by the regression-filtration method. Spectral dependences of the magnitude and phase of the amplitude reflection coefficient of the film (*b*). Vertical lines mark the wave numbers ν_j ($j = 0 \div 5$) satisfying the condition $\text{Im } r_X(\nu_j) = 0$. (*c*) Error of determination of the model refractive index $\Delta N(\nu) = N_X(\nu) - N_{\text{film}}(\nu)$

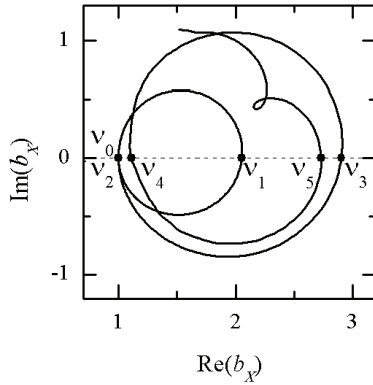


Fig. 4. Hodograph of the quantity $b_X(\nu)$ calculated by expression (13). The wave numbers ν_j ($j = 0 \div 5$) simultaneously satisfy the conditions $\text{Im } r_X(\nu_j) = 0$ and $\text{Im } b_X(\nu_j) = 0$

of the amplitude reflection coefficient of the film is completely determined:

$$r_X(\nu) = m_X(\nu) \exp[i\varphi_X(\nu)]. \quad (11)$$

Note the evident low-frequency asymptotic behavior of the phase, $\varphi_X(\nu \rightarrow 0) \rightarrow \pi$.

The dependence of the amplitude reflection coefficient on the thickness $d_3 = d_{\text{film}}$ and the dielectric permittivity $\varepsilon_3 = \varepsilon_{\text{film}}$ of the single-layer film is well known. Let us rewrite it in a different form. We introduce new variables: the ratio between the z -components of the wave vectors in the film and substrate,

$$x = \frac{q_3}{q_4} = \frac{\sqrt{\varepsilon_3 - \varepsilon_0 \sin^2 \alpha}}{\sqrt{\varepsilon_4 - \varepsilon_0 \sin^2 \alpha}}, \quad (12)$$

and the ratio between the amplitudes of the magnetic and electric fields in the gap near the film (with an accuracy to the parameter q_4),

$$b_X(\nu) = \frac{q_2}{q_4} \frac{1 - r_X(\nu)}{1 + r_X(\nu)}. \quad (13)$$

In terms of these variables, the boundary conditions (D3) at the gap-film interface are written in the form of a matrix equation for the variable $x(\nu)$:

$$\begin{vmatrix} b_X(\nu) & \cos \Phi(\nu) - ix \sin \Phi(\nu) \\ 1 & \cos \Phi(\nu) - \frac{i}{x} \sin \Phi(\nu) \end{vmatrix} = 0, \quad (14)$$

where $\Phi(\nu) = 2\pi\nu q_4 d_3 x(\nu)$.

In order to determine the unknown film thickness, let us consider the complex quantity $b_X(\nu)$ calculated

according to expression (13). Its hodograph is shown in Fig. 4. The roots ν_j ($j = 0 \div 5$) of the equation

$$\text{Im } b_X(\nu) = 0 \quad (15)$$

are shown by open circles in Fig. 4 and vertical lines in Fig. 3, *b*. The most interesting are the roots that are located in the film transparency interval. From Eq. (14), it follows that there is an interference resonance for them: $2\pi\nu_j q_3(\nu_j) d_3 = j\pi/2$. Moreover, for the “even” roots ν_{2m} with $m = 0, 1, 2, \dots$, we have $b_X(\nu_{2m}) = 1$, and the hodograph intersects the real axis at point 1. At the same time, for the “odd” roots ν_{2m+1} , the intersection of the hodograph with the real axis at the point $b_X(\nu_{2m+1}) = x^2(\nu_{2m+1}) = (q_3/q_4)^2$ can be used to determine the film thickness. For any “odd” root, the z -component of the wave vector in the film can be written as

$$q_3(\nu_{2m+1}) = q_4(\nu_{2m+1}) \sqrt{b_X(\nu_{2m+1})}.$$

Therefore, we obtain the following formula for the film thickness:

$$d_{3X} = \frac{2m + 1}{4\nu q_4(\nu_{2m+1}) \sqrt{b_X(\nu_{2m+1})}}. \quad (16)$$

Note also that any hodograph point $b_X(\nu)$ in the transparency interval lies on a circle, whose diameter connects two points on the real axis: 1 and $(q_3(\nu)/q_4(\nu))^2$.

Let us analyze the roots of Eq. (15) (Fig. 4). The trivial root $\nu_0 = 0$ testifies to the absence of a singularity in the absorption at low frequencies. The root ν_2 undoubtedly belongs to the film transparency interval, because, as follows from Eq. (14), the equality $b_X(\nu_2) = 1$ can take place only if $x(\nu_2)$ has a real value. Thus, we may assume that the root ν_1 also belongs to the transparency interval. At the same time, $b_X(\nu_4) \neq 1$, i.e. the root ν_4 belongs to the interval of film absorption. The intermediate root ν_3 is evidently located near the absorption boundary. The numerical calculation of the film dielectric constant following this scheme is based on the parameter d_{3X} corresponding to the film thickness. In the case of root ν_1 , formula (16) gives the value

$$d_{3X} = \frac{1}{4\nu_1 q_4(\nu_1) \sqrt{b_X(\nu_1)}} = 0.150004 \mu\text{m},$$

which practically coincides with the d_{film} -value used in the spectrum calculation.

Now, the matrix equation (14) contains only one unknown quantity, $x(\nu)$, which can be numerically determined in the whole spectral interval. The spectral dependences of the complex refractive index in the film, $N_X(\nu)$, and the corresponding dielectric permittivity $\varepsilon_X(\nu)$ are calculated according to definition (12) as follows:

$$N_X(\nu) = \sqrt{\varepsilon_X(\nu)} = \sqrt{\varepsilon_0 \sin^2 \alpha + x^2(\nu) q_4^2(\nu)}. \quad (17)$$

The result of calculations following this scheme is shown in Fig. 3, *c* in the form of the determination error for the model refractive index (5)

$$\Delta N(\nu) = N_X(\nu) - N_{\text{film}}(\nu).$$

One can see that both the real and imaginary parts of $N_{\text{film}}(\nu)$ are reproduced with an accuracy of about 10^{-3} in the whole spectral interval. An exception is a narrow interval of wave numbers $\nu = 3.7 \div 4 \mu\text{m}^{-1}$ near the upper end of the spectrum. The most probable reason for that is the Fourier filtering of low frequencies, which distorts the functions $w_m(\nu)$ and $w_a(\nu)$ to some extent near this end. A certain accuracy worsening (to $0.005 \div 0.007$) is observed in the interval $\nu = 2.4 \div 2.6 \mu\text{m}^{-1}$ and in a vicinity of the wave number $\nu = 3 \mu\text{m}^{-1}$. The origin of those errors has not been established yet.

3.4. Refinement of the gap thickness value

In Subsection 3.3, the inverse problem was solved by assuming that the gap thickness is known. The corresponding scheme of sequential calculations looked like the chain

$$\begin{aligned} d_{\text{gap}} &\xrightarrow{(10)} \varphi_X(\nu) \xrightarrow{(11)} r_X(\nu) \xrightarrow{(13)} b_X(\nu) \xrightarrow{(15)} \nu_1 \xrightarrow{(16)} d_{3X} \approx \\ &\approx d_{\text{film}} \xrightarrow{(14)} x(\nu) \xrightarrow{(17)} N_X(\nu) \approx N_{\text{film}}(\nu). \end{aligned} \quad (18)$$

The modern equipment, e.g., Aerotech nanopositioning stages [31], allows the distances and displacements to be controlled to an accuracy higher than $0.01 \mu\text{m}$, which seems to be sufficient for independent measurements of the gap thickness. However, the presence of the transparency interval for the film makes it possible to refine the gap thickness value exclusively by numerically analyzing the experimental data.

Let us assume that the calculation chain (3.3.4) contains an error δd_{gap} for the gap thickness from

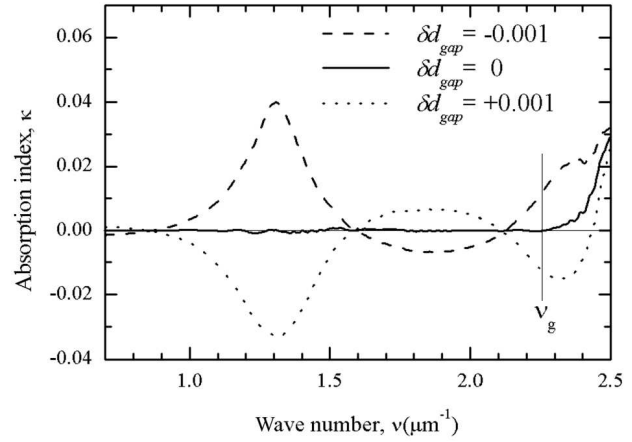


Fig. 5. Calculation results of the imaginary part of the refractive index for three values of the gap thickness error δd_{gap}

the very beginning. Then we obtain a chain of errors that can be depicted in the form

$$\begin{aligned} d_{\text{gap}} + \delta d_{\text{gap}} &\xrightarrow{(10),(11)} \dots \xrightarrow{(13),(15),(16)} d_{3X} = d_{\text{film}} + \\ &+ \delta d_{\text{film}} \xrightarrow{(14)} x(\nu) \xrightarrow{(17)} N_X(\nu) = N_{\text{film}}(\nu) + \delta N(\nu). \end{aligned}$$

As a result, a qualitative effect should manifest itself; namely, the imaginary part of the refractive index does not disappear in the transparency interval,

$$\text{Im } N_X(\nu) = \text{Im } \delta N(\nu) \neq 0.$$

Moreover, it will accept both positive and negative values. The latter are nonphysical in general, because it is assumed that the film does not amplify optical signals. To illustrate this effect, the results of calculations following the calculation scheme are exhibited in Fig. 5 in the form of the spectral dependences $\text{Im } \delta N(\nu)$ for three values of the gap thickness error $\delta d_{\text{gap}} = -0.001, 0, \text{ and } 0.001 \mu\text{m}$.

This observation laid the basis for the procedure aimed at the determination and refinement of the gap thickness value. First of all, the first approximation $d_{\text{gap}}^{(1)}$ is sought for the gap thickness, by linearly interpolating the dependence $\beta_X(\nu) = \beta_0 + 4\pi\nu d_{\text{gap}}^{(1)} \sqrt{\varepsilon_0} \cos \alpha$. The optimized value $d_{\text{gap}}^{\text{opt}}$ is determined in a narrow vicinity of $d_{\text{gap}}^{(1)}$, by minimizing the deviations of the imaginary part $\text{Im } N_X(\nu)$ from zero in the interval $\nu = 0.7 \div 1.7 \mu\text{m}^{-1}$, i.e. in the section of the transparency interval that contains

two sequential roots ν_1 and ν_2 . After the optimization, the values obtained for the gap thickness $d_{\text{gap}}^{\text{opt}}$ and the film thickness $d_{\text{film}}^{\text{opt}}$ were practically identical to the reference values: $|d_{\text{gap}}^{\text{opt}} - d_{\text{gap}}| \sim 10^{-6} \mu\text{m}$ and $|d_{\text{film}}^{\text{opt}} - d_{\text{film}}| \sim 10^{-6} \mu\text{m}$. After substituting the $d_{\text{gap}}^{\text{opt}}$ -value as the input parameter of chain (3.3.4), the determination error of the model refractive index did not change; it completely coincided with the results depicted in Fig. 3, c.

Hence, the assumption that the gap thickness value can be refined exclusively by numerically analyzing experimental data was confirmed. As a result, we have proved that, for a complete solution of the inverse problem in the case of a thin single-layer film, the experimental data for the normalized reflection spectrum $\rho_X(\nu)$ are enough. The corresponding solution procedure includes a number of sequential stages: the refinement of the gap thickness (Subsection 3.4), the determination of the film thickness (Eq. (16)), the solution of the matrix equation (14) for all spectral points, and the calculation of the spectral dependence of the complex refractive index of the film $N_X(\nu)$ (Eq. (17)).

4. Conclusions

In this work, we have put forward an idea that allows the phase of the amplitude reflection coefficient of the surface to be determined solely on the basis of data describing the normalized reflection spectrum obtained for an artificially created structure, namely, an interferometer, for which the researched surface is one of its sides. The procedure of normalization of the spectrum following the “moving specimen” principle is described, and a relation between the phase of short-period oscillations arising in the normalized spectrum owing to the gap between the interferometer sides and the phase of the amplitude reflection coefficient of the surface is demonstrated. The peculiarities of the artificially created structure allow the method of phase measurement to be called the “in-gap” spectroscopy.

We have demonstrated a numerical procedure, which allows the transformation of the normalized reflection spectrum into the spectral dependences of the reflection coefficient magnitude and phase, as well as analytical relations required for this purpose. In such a way, it is proved that the proposed measurement method allows the maximally complete information

about the specular reflection of light from the surface to be extracted. This ability distinguishes it from other optical methods, which can supply only an incomplete information.

A possibility of applying only the normalized reflection spectrum in order to solve the inverse problem and to determine the physical properties of the surface is examined on a simple example of a transparent insulator covered with an isotropic semiconductor film. We have obtained a simple matrix equation, which includes the complex reflection coefficient and the dielectric permittivity of the film. The film thickness can be found, by analyzing the reflection coefficient spectrum. Thereby, the solution of the inverse problem is reduced to an algebraic transformation of the normalized reflection spectrum into the physical parameters of the film. This fact advantageously distinguishes the proposed method against ellipsometry. For the latter, the solution of the inverse problem demands an optimization procedure, i.e. the search for physical parameters that would provide the best solution for the direct problem (the fitting of ellipsometric angles).

One may expect that, owing to extended experimental possibilities, the proposed method will be useful both for the characterization of more complicated films (including multilayer and anisotropic ones) and for the research of layered structures with interesting physical properties (inversion layers, surface plasmons, excitons, polaritons, and so forth).

APPENDIX

In Appendix, the system of matrix equations is presented, which describes the transmission of an *s*-polarized monochromatic plane wave through a system of plane-parallel nonmagnetic layers and which was used in the calculations. The configuration of the system is exhibited in Fig. 1. The *z*-axis is directed along the normal to the layers. Light falls at the angle α in the plane *xz*. Each *j*-th layer is located between the coordinates z_j and z_{j+1} and is characterized by the specific isotropic dielectric constant ε_j :

$$\varepsilon(z_j < z < z_{j+1}) = \varepsilon_j.$$

To describe the components (E_y, H_x) of the electromagnetic field in the *j*-th layer, let us introduce a two-component column vector $\mathbf{V}_j(z)$ [16, 32], so that

$$\begin{aligned} \begin{pmatrix} -H_x(z) \\ E_y(z) \end{pmatrix} \Big|_{z_j < z < z_{j+1}} &= e^{i2\pi\nu\sqrt{\varepsilon_0}\sin\alpha \cdot x} V_j(z) = \\ &= e^{i2\pi\nu\sqrt{\varepsilon_0}\sin\alpha \cdot x} \frac{1}{\sqrt{2}} \begin{pmatrix} q_j^{1/2} & -q_j^{1/2} \\ -1/2 & q_j^{-1/2} \end{pmatrix} U_j(z), \end{aligned} \quad (\text{D1})$$

where

$$U_j(z) = \begin{pmatrix} u_j(z) \\ u_j(z) y_j(z) \end{pmatrix} = \begin{pmatrix} a_j e^{i2\pi\nu q_j(z-z_j)} \\ a_{-j} e^{-i2\pi\nu q_j(z-z_j)} \end{pmatrix}$$

is the amplitude column vector describing the amplitudes of the incident, $u_j(z)$, and reflected, $u_j(z) y_j(z)$, waves; ν is the wave number; and $q_j = \sqrt{\varepsilon_j - \varepsilon_0 \sin^2 \alpha}$ is a dimensionless coefficient. It is evident that the product $\nu q_j = \nu \sqrt{\varepsilon_j - \varepsilon_0 \sin^2 \alpha}$ has the meaning of the wave vector z -component in the j -th layer. The ratio of wave amplitudes, $y_j(z)$, is called the amplitude reflection coefficient or, briefly, the reflection amplitude.

Within any layer, the amplitude vector is transformed as the matrix product

$$U_j(z') = \begin{pmatrix} e^{i2\pi\nu q_j(z'-z)} & 0 \\ 0 & e^{-i2\pi\nu q_j(z'-z)} \end{pmatrix} U_j(z) = T(q_j, z' - z) U_j(z). \quad (D2)$$

According to the boundary conditions, the field vector does not change, when crossing the interface:

$$V_{j-1}(z_j) = V_j(z_j). \quad (D3)$$

As a result, the amplitude vector is transformed as the matrix product

$$U_{j-1}(z_j) = \frac{1}{2\sqrt{q_{j-1}q_j}} \begin{pmatrix} q_{j-1} + q_j & q_{j-1} - q_j \\ q_{j-1} - q_j & q_{j-1} + q_j \end{pmatrix} U_j(z_j) = R(q_{j-1}, q_j) U_j(z_j). \quad (D4)$$

With the help of those definitions, let us determine expressions that are used throughout the paper.

1. Amplitude of reference reflection (Fig. 1, b)

In the absence of the substrate and the film, there is only the incident wave in medium 2 (air). Therefore, $y_{\text{win}}^{\text{ref}}(z_2)$, i.e. the amplitude ratio in medium 1 (window), satisfies the equation

$$u_1(z_2) \begin{pmatrix} 1 \\ y_{\text{win}}^{\text{ref}}(z_2) \end{pmatrix} = U_1(z_2) = R(q_1, q_2) U_2(z_2) = \frac{1}{2\sqrt{q_1 q_2}} \begin{pmatrix} q_1 + q_2 & q_1 - q_2 \\ q_1 - q_2 & q_1 + q_2 \end{pmatrix} u_2(z_2) \begin{pmatrix} 1 \\ 0 \end{pmatrix}.$$

From whence,

$$y_{\text{win}}^{\text{ref}}(z_2) = \frac{q_1 - q_2}{q_1 + q_2} = r_{12}. \quad (D5)$$

2. Relationship between the reflection amplitude of the "Film-in-Gap" structure and the amplitude reflection coefficient of the film $r_{\text{film}}(\nu)$ (Fig. 1, a)

The amplitude vector in the gap near any film (single or multilayer) has the form

$$U_2(z_3) = u_2(z_3) \begin{pmatrix} 1 \\ r_{\text{film}}(\nu) \end{pmatrix}.$$

Therefore, the amplitude ratio $y_{\text{win}}^{\text{FiG}}(z_2)$ in medium 1 (window) satisfies the equation

$$u_1(z_2) \begin{pmatrix} 1 \\ y_{\text{win}}^{\text{FiG}}(z_2) \end{pmatrix} = U_1(z_2) = R(q_1, q_2) T(q_2, -d_2) u_2(z_3) \begin{pmatrix} 1 \\ r_{\text{film}}(\nu) \end{pmatrix}.$$

As a result, the reflection amplitude of the structure looks like

$$y_{\text{win}}^{\text{FiG}}(z_2) = \frac{r_{12} + r_{\text{film}}(\nu) e^{i4\pi\nu q_2 d_2}}{1 + r_{12} r_{\text{film}}(\nu) e^{i4\pi\nu q_2 d_2}}. \quad (D6)$$

3. Numerical calculation of the normalized reflection spectrum of the single-layer "Film-in-Gap" structure

The amplitude vector in the substrate is formed by the incident wave only,

$$U_4(z_4) = u_4(z_4) \begin{pmatrix} 1 \\ 0 \end{pmatrix}.$$

In this case, the reflection amplitude of the structure, $y_{\text{win}}^{\text{FiG}}(z_2)$, is determined from the equation

$$u_1(z_2) \begin{pmatrix} 1 \\ y_{\text{win}}^{\text{FiG}}(z_2) \end{pmatrix} = R(q_1, q_2) T(q_2, -d_2) \times R(q_2, q_3) T(q_3, -d_3) R(q_3, q_4) u_4(z_4) \begin{pmatrix} 1 \\ 0 \end{pmatrix}, \quad (D7)$$

and the normalized reflection spectrum is evidently calculated as the ratio

$$\rho(\nu) = \left| \frac{y_{\text{win}}^{\text{FiG}}(z_2)}{y_{\text{win}}^{\text{ref}}(z_2)} \right|^2. \quad (D8)$$

1. I.V. Masol, V.I. Osinskii, O.T. Sergeev. Information Nanotechnologies (Macros, 2011) (in Russian).
2. A.A. Goncharov, A.N. Dobrovolskii, E.G. Kostin, I.S. Petrik, E.K. Frolova. Optical, structural, and photocatalytic properties of nanosize titanium dioxide films deposited in magnetron discharge plasma. *Zh. Tekhn. Fiz.* **84**, No. 6, 98 (2014) (in Russian).
3. A.A. Goncharov, A.N. Evsyukov, E.G. Kostin, B.V. Steetsenko, E.K. Frolova, A.I. Shchurenko. Synthesis of nanocrystalline titanium dioxide films in a magnetron-type cylindrical gas discharge and their optical characterization. *Zh. Tekhn. Fiz.* **80**, No. 8, 127 (2010) (in Russian).
4. V. Lucarini, J.J. Saarinen, K.-E. Peiponen, E.M. Vartiainen. *Kramers-Krönig Relations in Optical Materials Research* (Springer, 2005).
5. R. Kitamura, L. Pilon, M. Jonasz. Optical constants of silica glass from extreme ultraviolet to far infrared at near room temperature. *Appl. Opt.* **46**, 8118 (2007).
6. S.P. Lyashenko, V.K. Miloslavskii. A simple method for determining the thickness and optical constants of semiconductor and dielectric layers. *Opt. Spektrosk.* **16**, 151 (1964) (in Russian).

7. A.S. Valeev, Determination of optical constants of thin weakly absorbing layers. *Opt. Spektrosk.* **15**, No. 4, 111 (1963) (in Russian).
8. R. Swanepoel. Determination of the thickness and optical constants of amorphous silicon. *J. Phys. E* **16**, 1214 (1983).
9. A.R. Forouhi, I. Bloomer. Optical dispersion relations for amorphous semiconductors and amorphous dielectrics. *Phys. Rev. B* **34**, 7018 (1986).
10. A.R. Forouhi, I. Bloomer. Optical properties of crystalline semiconductors and dielectrics. *Phys. Rev. B* **38**, 1865 (1988).
11. G.E. Jellison, F.A. Modine. Parameterization of the optical functions of amorphous materials in the interband region. *Appl. Phys. Lett.* **69**, 371 (1996).
12. A. Rothen. The ellipsometer, an apparatus to measure thickness of thin surface films. *Rev. Sci. Instrum.* **16**, 26 (1945).
13. R.M.A. Azzam, N.M. Bashara. *Ellipsometry and Polarized Light* (North-Holland, 1977).
14. *Handbook of Ellipsometry*. Edited by H.G. Tompkins, E.A. Irene (W. Andrew Publ., 2005).
15. H. Fujiwara, *Spectroscopic Ellipsometry: Principles and Applications* (Wiley, 2007).
16. I.S. Petryk, O.V. Turchin, O.K. Frolova. Estimation of the measurement accuracy of a thin non-absorbent film parameters using ellipsometry at various incidence angles. *Ukr. Fiz. Zh.* **51**, 623 (2006) (in Ukrainian).
17. T.M. Kreis, W.P.O. Jüptner. Principles of digital holography. In *Proceedings of the 3rd International Workshop on Automatic Processing of Fringe Patterns, Bremen, Germany, September 15–17, 1997* (Akademie, 1997), p. 353.
18. D. Carl, B. Kemper, G. Wernicke, G. von Bally. Parameter-optimized digital holographic microscope for high-resolution living-cell analysis. *Appl. Optics* **43**, 6536, (2004).
19. M.K. Kim. *Digital Holographic Microscopy: Principles, Techniques, and Applications* (Springer, 2011).
20. M. Liebling, T. Blu, M. Unser. Complex-wave retrieval from a single off-axis hologram. *J. Opt. Soc. Am. A* **21**, 367 (2004).
21. B. Hecht, B. Sick, U.P. Wild *et al.* Scanning near-field optical microscopy with aperture probes: Fundamentals and applications. *J. Chem. Phys.* **112**, 7761 (2000).
22. A. Nesci. *Measuring Amplitude and Phase in Optical Fields with Sub-Wavelength Features*. PhD thesis (Univ. of Neuchatel, 2001).
23. K. Creath. Phase-measurement interferometry techniques. *Progr. Optics* **26**, 349 (1988).
24. H. Schreiber, J.H. Bruning. Phase shifting interferometry. In *Optical Shop Testing*. Edited by D. Malacara (Wiley, 2007), chap. 14.
25. I. Yamaguchi, T. Zhang. Phase-shifting digital holography. *Opt. Lett.* **22**, 1268 (1997).
26. G.E. Sommargren. *Interferometric Wavefront Measurement*. US Patent 4, 594, 003 (1986).
27. J. Schmit, K. Creath, J.C. Wyant. Surface profilers, multiple wavelength, and white light interferometry. In *Optical Shop Testing*. Edited by D. Malacara (Wiley, 2007), chap. 15.
28. P.J. de Groot, Interference microscopy for surface structure analysis. In *Handbook of Optical Metrology: Principles and Applications*. Edited by T. Yoshizawa (CRC Press, 2015), chap. 31.
29. A.F. Fercher. Optical coherence tomography. *J. Biomed. Opt.* **1**, 157 (1996).
30. I.H. Malitson. Interspecimen comparison of the refractive index of fused silica. *J. Opt. Soc. Am.* **55**, 1205 (1965).
31. <http://www.aerotech.com/product-catalog/stages.aspx>.
32. M. Born, E. Wolf. *Principles of Optics: Electromagnetic Theory of Propagation, Interference and Diffraction of Light* (Cambridge Univ. Press, Cambridge, 1999).

Received 23.03.16.

Translated from Ukrainian by O.I. Voitenko

O.V. Турчин

СПЕКТРОСКОПІЯ У ЗАЗОРІ: ФАЗА
ВІДБИТОЇ ХВИЛІ І ХАРАКТЕРИЗАЦІЯ ПЛІВОК

Резюме

Оптичні методи характеристики поверхні спираються на вимірювання або відношення комплексних коефіцієнтів відбивання для ортогональних поляризацій світла (еліпсометрія), або магнітуди цих коефіцієнтів, що дозволяє розв'язати обернену проблему, тобто обчислити параметри поверхні (такі як кількість, товщина та проникність плівок), шляхом їх оптимізації. З метою збільшити кількість величин, що вимірюються експериментально, у роботі пропонується метод визначення фази відбитого світла шляхом аналізу спектральних особливостей світла, відбитого від плоскопаралельного зазору, одну з граней якого утворює досліджувана поверхня. Показано, яким чином нормований спектр, отриманий в результаті процедури “рухомого зразка”, може бути конвертовано у спектральну залежність магнітуди і фази коефіцієнта відбивання. Продемонстровано, що знання комплексного коефіцієнта відбивання зводить обернену проблему до відновлення діелектричної проникності одношарової плівки до розв'язку лінійного матричного рівняння. Це вигідно відрізняє метод у порівнянні з еліпсометрією, для якої не існує прямої трансформації еліпсометричних кутів у фізичні параметри плівки.